Gut Microbiome Composition and Metabolomic Profiles of Wild and Captive Chinese Monals (Lophophorus Lhuysii)

Dandan Jiang
Chengdu research base of giant panda breeding
Xin He
Chengdu research base of giant panda breeding
Marc Valitutto
Chengdu research base of giant panda breeding
Li Chen
Sichuan Fengtongzhai National Nature reserve administration
Qin Xu
Chengdu research base of giant panda breeding
Ying Yao
Chengdu research base of giant panda breeding
Rong Hou
Chengdu research base of giant panda breeding
Hairui Wang (pandaharry@panda.org.cn)
Chengdu research base of giant panda breeding

Research

Keywords: Chinese monal, Microbiome, Metabolite, Gut microbiota, Feces

Posted Date: June 8th, 2020

DOI: https://doi.org/10.21203/rs.3.rs-32587/v1

Version of Record: A version of this preprint was published on December 3rd, 2020. See the published version at https://doi.org/10.1186/s12983-020-00381-x.

Abstract

Background The Chinese monal (*Lophophorus lhuysii*) is an endangered bird species, with a wild population restricted to the mountains of southwest China, and only one known captive population in the world. We investigated the fecal microbiota and metabolomics of wild and captive Chinese monals to explore differences and similarities in nutritional status and digestive characteristics. An integrated approach combining 16S ribosomal rRNA (16S rRNA) gene sequencing and ultra-high performance liquid chromatograph (UHPLC) based metabolomics were used to examine the fecal microbiome composition and the metabolomic profile of Chinese monals.

Results: The results showed that the alpha diversity of gut microbes in the wild group were significantly higher than that in the captive group and the core bacterial species in the two groups showed remarkable differences at all levels. Metabolomic profiling revealed a concurrent difference, mainly related to galactose, starch and sucrose metabolism, fatty acid, bile acid biosynthesis and bile secretion. Furthermore, these metabolites in difference are have a strong correlation with the main microbe in genus level.

Conclusions: Various factors related to diet and environmental conditions played a crucial role in shaping the gut microbiome composition and metabolomic profile. Through this study, we have established a baseline for a normal gut microbiome and metabolomic profile for wild Chinese monals, thus allowing us to evaluate if differences seen in captive specimens has an impact on their overall health and reproduction.

Background

The Chinese monal (*Lophophorus lhuysii*) belongs to the order Galliformes, family Phasianidae, distributed in the mountains of southwest China at an elevation of 3,000 to 4,900 meters [1]. It is an endemic bird species of China, which has been listed as endangered by the Convention on International Trade in Endangered Species of Wild Fauna and Flora (CITES)[2], classified as a vulnerable species on the International Union for Conservation of Nature (IUCN)red list [3], and has been protected in China as a first-class, nationally-protected wildlife species since 1989 [1]. There has been limited success with establishing captive breeding groups of Chinese monals throughout the world, the reason for which is not entirely clear [4]. At present, the world's only captive collection exists in the Fengtongzhai National Nature Reserve in Sichuan, China, with only 23 individuals as of early 2020. The IUCN states the wild population of Chinese monal continues to decrease with research needed to understand their ecology and threats to their livelihood (Available at https://www.iucnredlist.org/species/22679192/30181918). However, given the limited access to captive and wild Chinese monals, few studies have been conducted in any field [4]. With a declining population, it is imperative to learn more about the Chinese monal to ensure a healthy existence of the species.

The gut microbiota is recognized as a coevolutionary partner with an ecosystem that is metabolically adaptable, rapidly renewable, and metabolically flexible [5, 6]. It performs numerous beneficial functions for the host, such as nutrient acquisition, immunomodulation and physiogenesis in response to profound lifestyle changes [7, 8]. Numerous factors influence the unique and variable community of gut microbiota present in each individual, such as host's age [9], diet composition (Guan et al. 2017), social interactions [11], gut morphology[9] and health status [12]. Thus, the study of intestinal microbial activity is helpful to understand the health and nutritional status of the host.

Meanwhile, the gut microbiota is closely related to the host's metabolic phenotype, which is a product of resident microbial communities integrated with host cells [13]. Any differences in the microbial community may have a significant effect on the metabolite profiles of the host's blood, urine, and fecal extracts [14], the influence of which can be explored through untargeted metabolomics that offers new opportunities to investigate individual needs, foods and nutritional functions [5]. The combined study of fecal 16S ribosomal rRNA (16S rRNA) sequencing and untargeted metabolomics promises to uncover the inherent associations between the microbiome and the host metabolic phenotypes [14]. The two techniques have been used to elucidate the relationship between environmental and ecological factors and gut microbes [15], as well as changes in gut microbes and host metabolic phenotypes in the context of different food composition [16, 17].

There are currently reports on the use of fecal 16S rRNA sequencing in wildlife, including birds [12, 18–20] and mammals [10, 11, 21, 22], these studies all have observed considerable differences between wild and captive individuals, but few studies on untargeted metabolomics in wild animals, especially birds, have been reported. Therefore, the objectives of the present study were to investigate the fecal microbiota and metabolomics of wild (WCM) and captive Chinese monal (CCM).

Results

Monal species identification

There were 6 and 37 samples of the feces in Yuancaopo and Hongshanding belonging to the Chinese monal, respectively, according to the species identification. The remaining samples were identified as 22 blood pheasants (*Ithaginis cruentus*), 6 temminck's tragopan (*Tragopan temminckii*), and 8 samples without amplification results.

Microbial Community Composition

A total of 1,466,455 high-quality reads with an average sequencing depth of 35,767 ± 1,265 reads per WCM fecal sample was conducted and classified into 2,132 operational taxonomic units (OTUs). Whereas, 580,736 high-quality reads with an average sequencing depth of 36,296 ± 1,062 reads per CCM fecal sample was conducted and classified into 4,899 OTUs. The number of OTUs present in both the wild and captive groups was 1,234, with 898 unique OTUs in the wild group, and 3,665 unique OTUs in

the captive group (Fig. 2A). The species accumulation curves (Fig. 1A) and rank abundance curves (Fig. 1B) of the WCM and CCM fecal samples convey the richness and evenness of the microbial species in the samples, and the curve had reached a plateau. These findings demonstrated that the sequencing data was acceptable and reflected the diversity of the gut microbiome.

The gut microbiome alpha diversity indexes in WCM were significantly higher than that of the CCM ($P_{Shannon}$ = 0.0066, P_{Chao1} = 0.000011) at the microbial species level. The discrepancy between the WCM and CCM was further analyzed via the partial least squares discrimination analysis (PLS-DA) plot as illustrated in Fig. 2B. The distance between the orange and blue color markers demonstrated a unique bacterial community structure in WCM vs. CCM, suggesting that there was a significant difference in gut microbial composition between the groups.

The predominant microbial phyla identified included *Proteobacteria* (49.6%), *Firmicutes* (23.8%), *Actinobacteria* (8.7%) in the wild group, and *Firmicutes* (53.5%), *Proteobacteria* (32.0%), *Cyanobacteria* (6.0%) in the captive group. At the genus level, *Ochrobactrum* (12.1%) dominated the wild Chinese monal gut microbiome, followed by *Faecalitalea* (9.0%), and *Acinetobacter* (6.7%), whereas, for captive individuals, *Escherichia-Shigella* (16.7%), *Enterococcus* (16.0%) and *Streptococcus* (6.3%) were primarily identified. The top 20 species for each group at phylum and genus level were shown in Fig. 3A and 3B, respectively.

Microbiome–metabolome Association

Strong associations between microbiome composition (at genus level) and metabolite perturbations were revealed by a Mantel test (r = 0.825,P = 0.001). Significant correlations could be detected between the fecal microbiome and metabolite based on Spearman correlation coefficients (r > 0.5 or r < -0.5, P < 0.05) [15]. Among the metabolites, fatty acids, bile acid derivatives, and carbohydrate were involved in more than half of the metabolic pathways. Metabolites that were remarkably different were highly correlated with microorganisms. The correlations between specific fecal metabolites and the top 10 most common fecal bacteria genera were shown in Fig. 6A.

Ochrobactrum, *Faecalitalea*, *Acinetobacter*, *Pelomonas*, *Ralstonia* (F1) were the dominant genera of the wild group, and *Escherichia-Shigella*, *Enterococcus*, *Peptoclostridium* (F2) *Streptococcus* and *Clostridium_sensu_stricto_1* were for the dominant genera of the captive individuals. The results showed fatty acids (linoleic acid, oleic acid, palmitic acid, stearic acid, 2E-eicosenoic acid), and bile salt (chenodeoxycholate) were higher in the feces of the CCM and negatively correlates with F1, but mainly positively correlates with F2. However, carbohydrate (stachyose, galactinol, sucrose, and raffinose), bile acid (taurodeoxycholic acid, tauroursodeoxycholic acid) and bile salts (taurochenodeoxycholate, taurocholate) were higher in the feces of WCM and mainly negatively correlates with F2, but positively correlates with F1. Remarkably, 5-hydroxyindoleacetic acid and indole-2-carboxylic acid, which increased 113.3 and 295.7-fold, respectively, in CCM, negatively correlates with F1 but positively correlates with F2. Moreover, Sinigrin was decreased 3,189.2-fold in the CCM, and positively correlates with F1 but negatively

correlates with F2. There was no significant correlation between cellobiose and F1, F2 (Fig. 6A), while cellobiose was positively correlated with *Enterorhabdus* and negatively correlated with *Arthrobacter*, *Pseudomonas* and *Paenibacillus* (Fig. 6B).

Discussion

Through fecal analysis, we studied the gut microbiome structure and the metabolomic profiles in both wild (WCM) and captive Chinese monals (CCM). The results of this research indicated distinct differences of the fecal bacterial communities between the two groups, furthermore, we identified significant correlations between the fecal microbiota and metabolites.

The levels of microbiome alpha and beta-diversity from WCM were significantly higher than CCM, indicating a more diverse microbial community in the wild population. These differences may be the result of differences in diet composition, geographical ranges, energy utilization, climate conditions, and stress exposure in the WCM vs. the CCM [9, 11].

Proteobacteria was the dominant phylum in the feces of WCM followed by *Firmicutes*, while *Firmicutes* was relatively more abundant than *Proteobacteria* in the feces of the captive group. The characterization of gut bacteria in several studies reveals a dominance of *Firmicutes* and *Bacteroidetes*, a feature which appears to be typical for birds. The dominance of these phyla has been described in the ceca of turkeys (*Meleagris gallopavo*) [18], the feces of penguins (*Spheniscidae*) [23] and Japanese quail (*Coturnix japonica*) [24], as well as in the crop of hoatzin (*Opisthocomus hoazin*) [25]. However, one study reports that *Proteobacteria* and *Firmicutes* are the dominant phyla in the feces of the Lady Amherst's pheasant (*Chrysolophus amherstiae*), Reeves's pheasant (*Syrmaticus reevesii*), and Cabot's tragopan (*Tragopan caboti*) [26], which is more consistent with our observations of the microbiome composition in the Chinese monal. Moreover, *Bacteroidetes* just accounted for 3.8% and 1.6%, respectively, in the WCM and CCM unlike what was observed in the turkey, penguin, quail, and hoatzin studies. Based on the results of this study, it would appear that the gut microbial composition of the Chinese monal is most reflective of that which has been detected in other species of the family Phasianidae; however, in the aforementioned cited research only two samples per group were collected and study details are lacking which highlights the need for further research on this subject.

A large diversity of gut microbes has been described as adaptive and beneficial, with diet being considered one of the most critical factors shaping gut microbial structures. The Chinese monal is an omnivorous bird. For wild populations, food is scarce in the winter months, due to their natural environment being at a high altitude and low temperatures. Whereas, the small captive population of monals receives a relatively steady diet with no change in environment except for exposure to outdoor seasonal climate conditions. Our results indicated a high abundance of *Proteobacteria* in WCM. *Proteobacteria* have greatly variable morphology and versatile functions [27], previous studies have demonstrated that increased an richness of *Proteobacteria* in the gut microbial flora is mainly related to energy accumulation [28–30], and is more abundant when the host animal has prolonged exposure to

cold climates [29]. We suspect our findings in WCM may be in response to their comparatively complex dietary composition, as well as to help them with cold weather and scarce food to get more energy.

In contrast to WCM, *Firmicutes* was identified as the dominant bacteria phylum in CCM. Compared with the WCM, we suspect captive individuals are fed a diet with a comparatively higher lipid content. Diet composition, as indicated in Table 1 showed a 6.2% crude fat in the commercial pelleted feed, which provides the base of the diet, in addition to corn which contains 3.6–5.3% crude fat (The data provided at the China Feed-database Information Network Centre: http://www.chinafeeddata.org.cn/picture/pdf/CFIC2019_1.pdf). In a 2014 study, mice were fed a high-fat diet, and the *Firmicutes: Bacteroidetes* ratio in mice gut microbiome increased after three weeks, with the abundance of *Firmicutes* increased and *Bacteroidetes* depleted [31]. This finding is in accordance with many former studies, suggesting that a high-fat content in diet is one of the primary factors responsible for changes observed in gut microbe composition [7, 32]. Thus, the increased abundances of *Firmicutes* and the *Firmicutes*: *Bacteroidetes* ratio in CCW group (CCM 33.45 versus WCM 6.25) is likely the result of a higher lipid content in the diet.

Concerning the metabolome, we detected 58 significant metabolites that associated with 20 metabolic pathways. We found that a significantly higher fatty-acid content in feces of the CCM was related to unsaturated fatty acid and fatty acid biosynthesis. A previous study found that different dietary triacylglyceride composition has an influence on fatty acid content in the feces of human neonates[33]. Thus, our finding may be related to the nutrient composition of the diet, which contains a higher level of fat and a different lipid composition than what wild specimens are likely consuming. Otherwise, our results showed that the primary microbial genera in Chinese monal feces are significantly related to the metabolites we identified; therefore, microbial metabolism is an essential aspect that needs to be evaluated. Microbial biosynthesis of fatty acid may be due to cellular structure or storage, de novo synthesis from glucose, or incorporation of exogenous fatty acids directly into lipid structures [34, 35].

Table 1
Nutrient levels of commercial pellet feed (as fed basis, %)

Component	Water	Crude fat	Crude fiber	Crude protein
%	11.1	6.2	2.9	17.4

The content of metabolites in the feces relating to bile acid biosynthesis and bile secretion had a statistically significant difference between the WCM and CCM. Our results showed differences in metabolism of bile acid, an important component of bile, which plays a role in digestion and metabolism of dietary lipids and cholesterol [36, 37]. Chenodeoxycholate, taurochenodeoxycholate and taurocholate are bile salts that are hydrolyzed into free bile acids by bile salt hydrolase [38]. Chenodeoxycholate amount was higher in the feces of CCM, whereas taurochenodeoxycholate and taurocholate were more abundant in the WCM. Taurodeoxycholic acid and tauroursodeoxycholic acid are taurine conjugated bile acids that were expectedly more abundant in the feces of WCM. The type of bile salt that is most abundant may reflect how the corresponding bile acids play a major role in digestion which is dependent

on the dietary composition of each individual bird [39]. In the wild, Chinese monals primarily consume seeds and roots of shrubs in the winter when food is scarce, but they also consume a small amount of moss, earthworms and insect pupa [40, 41]. High concentrations of total non-structural carbohydrate (TNC) reserves are usually found in root tissues of plants [42–44], and may serves as one of the main energy sources for WCM. Because of the seed consumption, the WCM also need to secrete bile acids for fat digestion thus providing another valuable energy source. We also found a high correlation between the bile acid metabolites and gut microbial flora. There exists a mutual regulation between intestinal microbes and bile acids, for microbiome structure appear to be a major regulator of bile acid pool size and composition [45]. Kim G et. al. (2005) found that several bacterial genera in *Firmicutes* and *Actinobacteria* can hydrolyze bile salt [38], among which *Enterococcus* was significantly related to the above metabolites in this study.

A significantly higher abundance of carbohydrates was found in the feces of WCM as opposed to the CCM, including galactinol, raffinose, stachyose, sucrose, and cellobiose. In plants, raffinose and stachyose are oligosaccharides synthesized from sucrose, subsequently galactitol and galactose are also involved [46]. Animals don't secrete enzymes that utilize raffinose-series oligosaccharides, which are likely to be digested by microbial enzymes at the end of the gastrointestinal tract [47]. Coon et al. (1990) reported that ileal digestibility of raffinose and stachyose was less than 1.0% in roosters; however, the digestibility, determined with excreta collection, reached 90.5% and 83.8%, respectively [48]. Previous studies have also indicated several Passerine bird species have a low digestibility of sucrose [49, 50] as fecal sugar content increased after consuming sucrose solutions [50]. Cellobiose is an important hydrolytic product of cellulose degradation [51]. Plants contain significant quantities of cellulose, which is difficult to naturally digest by most birds species, but can be utilized by bacteria inhabiting the intestinal tract, especially within the ceca [52]. Yuzhang Wang (2007) reported that the cecum of the Chinese monal is well developed, accounting for 24.09% of the total length of the intestine [53], which may help the species utilize cellulose and other indigestible components of the diet. Microorganisms in genus that have significant positive correlation with these metabolites may play a big role in these processes.

Indole-containing metabolites were significantly different in fecal samples of CCM, such as 5-hydroxyindoleacetic acid (5-HIAA) and indole-2-carboxylic acid, which are nearly 100 and 300 times higher than that in the wild, respectively. Indole and its derivatives widely exist in animals, microorganisms and plants [54], and are the main metabolites of serotonin [55]. Degg et. al. (2002) found that excretion of indole containing metabolites, such as 5-HIAA, increased after humans ingested high serotonin-containing foods including tomatoes, bananas, etc. [56]. Our results which indicate higher levels of 5-HIAA and indole-2-carboxylic acid in CCM feces is likely associated with the incorporation of tomatoes in their routine diet. These two altered indole-containing metabolites were also highly correlated with fecal microbial flora. Previous studies have suggested that intestinal bacteria can conversion of tryptophan to indole through enzymatic processing, then form indole-containing metabolites [37, 57]. These studies showed that metabolic processes in intestinal bacteria are essential for the synthesis of indole-containing metabolites, therefore, it may be a specific indicator of intestinal bacteria differences.

Finally, the last metabolite with a significant difference observed between the two groups is sinigrin (2-propenyl glucosinolate). Sinigrin was several thousand times higher in the feces of WCM than that observed in CCM. Sinigrin, which is enriched in plants such as cruciferous vegetables, leaf mustard, and horseradish, has been associated with carbohydrate regulation and lipid metabolism and has also been shown to have anti-neoplasia and anti-microbial properties [58]. In vitro experiments confirmed that sinigrin was degraded by rat intestinal microbiota [54]. *Enterococcus* and *Bacteroides* in the human intestine can degrade glucosinolates [59], and have a significant positive correlation with sinigrin in this study. Therefore, based on our findings of high levels of sinigrin in WCM feces, we can speculate that the diet of WCM also contains a large amount of sinigrin. Although the intestinal flora plays a role in the digestion process, it is more excreted through feces.

Conclusion

This is the first study to evaluate the fecal microbiome and the fecal metabolic profiles in the Chinese monal. The results clearly demonstrate the differences of the gut bacterial composition and metabolism of the host and microbiome between wild and captive Chinese monals. The results of this study, will without a doubt, enhance our knowledge of wild and captive Chinese monals which may help guide recommendations that will affect the health and fecundity of birds in the captive breeding program. Further studies are required to determine if there is a difference in the fecal microbiome and `metabolic profiles in spring and summer months when the dietary composition is likely to change.

Methods

Birds selected, study site and sample collection

Samples were collected from October to December of 2018 at Baoxing Fengtongzhai National Nature Reserve in Sichuan Province, China. Fecal samples from the wild were collected at two research sites, located on two mountains: Yuancaopo (30°34'38"-30°35'3"N, 102°48'15"- 102°49'57"E) and Hongshanding (30°37'39"- 30°37'46"N, 102°54'57"- 102°55'3"E). Samples that appeared fresh (e.g. still wet) were collected at an altitude of 3223.7 to 3568.7 meters, and a temperature of -17 ºC – 5 ºC. In Yuancaopo and Hongshanding, 49 and 42 samples were collected, respectively.

In November 2018, fecal samples of 11 captive birds (3 males and 8 females) were collected at the Chinese Monal Conservation and Research Center, where the altitude is 1582.0 meters and the temperature range from 9 ºC – 13 ºC. These monals are maintained in four enclosures, with three enclosures containing one male each paired with one or two females, while one enclosure contains only three sub-adult females. Feces was collected by placing clean cardboard beneath the nightly roosting perches, overnight. The following morning at 8 AM, four fecal samples per enclosure were collected from the cardboard with an attempt to collect feces with varying colors and shapes.

Approximately 1 g of fecal material was collected from the central section of each fecal dropping, from both wild and captive animals, and placed into 1.5 mL sterile collection tubes (Corning, New York, USA) and immediately frozen in liquid nitrogen. Thereafter, the samples were shipped to the Chengdu Research Base of Giant panda Breeding within 24 h., where they were stored at -80 ºC for subsequent analysis.

Measurement of the main components of the commercial pellet feed

The commercial pellet (New hope group, Chengdu, China) being fed to the CCM was analyzed to measure the primary nutritional components according to Chinese national standards. Moisture was determined by direct drying method [60]. Crude fat was determined by petroleum ether extraction method [61]. Crude protein was determined by Kjeldahl method [62]. Crude fiber was determined by Soxhlet extraction method [63].

Monal Species Identification

Genomic DNA was isolated from the fecal samples using the TIANamp Micro DNA Kit (Tiangen, Beijing, China) following the manufacturer's instructions. The DNA was amplified using cytochrome *b* (Cyt *b*) gene primers; forward: 5'-ACATTGGACGCGGCCTCTAC-3' and reverse: 5'-GTGGGCGAAATGTTATGGTT-3'. PCR products were separated by electrophoresis in a 1% agarose gel, then recovered using the AxyPrep DNA gel recovery kit (Axygen, California, USA). The purified PCR products were sequenced using an ABI3730-XL genetic sequencer (Applied Biosystems, Foster City, CA, USA). Genetic sequencing data were blasted against the nucleic acid database of the National Center for Biotechnology Information (NCBI) using the Basic Local Alignment Search Tool (BLAST) program. Species identification was selected based on results that returned a BLANK % sequence similarity result.

16s Rrna Microbial Community Analysis

The total DNA was extracted from fecal samples using the DNeasy PowerSoil Kit (QIAGEN, Inc. Netherlands), using their designated protocol. The V4-V5 region of the 16S rRNA gene was PCR amplified using the forward primer 515 F: 5'-GTGCCAGCMGCCGCGGTAA-3' and the reverse primer 907 R: 5'-CCGTCAATTCMTTTRAGTTT-3'. Before being pooled, PCR amplicons were purified with Agencourt AMPure Beads (Beckman Coulter, Indianapolis, IN, USA), quantified using the PicoGreen dsDNA Assay Kit (Invitrogen, Carlsbad, CA, USA), and finally, paired-end sequencing with 2 × 300 bp read lengths was performed using the Illumine MiSeq platform with MiSeq Reagent Kit v3 at Shanghai Personal Biotechnology Co., Ltd (Shanghai, China).

The raw sequencing data were processed using the Quantitative Insights Into Microbial Ecology (QIIME, v1.8.0) software package. The low-quality sequences were filtered through criteria as previously described [64], and following chimera detection, the remaining high-quality sequences were clustered into OTUs with a threshold of 97% sequence similarity. OTU taxonomic classification was conducted via

BLAST searching the representative sequences set against the Greengenes Database [65] using the best hit [66].

Sequence data analyses were primarily calculated using QIIME and R packages (v3.2.0). Generated OTU-level ranked abundance curves to compare the richness and evenness of OTUs among samples. Venn diagram was obtained to visualize the mutual and unique OTUs between groups using R package “VennDiagram”. Alpha diversity was performed and discrepancies analyzed between the two groups using the wilcoxon test. Beta diversity analysis was performed to investigate the structural variation of microbial communities across samples using UniFrac distance metrics [67] and visualized via PLS-DA. The microbiota compositional profiles could be achieved at different taxonomic levels, including phylum, class, order, family and genus, wherewith the taxa abundances at these levels were statistically compared among samples or groups by Metastats [68].

Metabolomic Analyses

Nine samples were selected from WCM and CCM, respectively, for untargeted metabolomics analyses, which was performed with liquid chromatography/mass spectrometry (LC/MS). An Agilent 1290 Infinity LC ultra-high performance liquid chromatograph (UHPLC) (Agilent, Palo Alto, USA), after sample pre-treatment. The mass spectrometer (MS) used was a Triple TOF 6600 system (AB/Sciex, Foster City, USA) equipped with an electrospray ionization (ESI) source in positive (ESI+) and negative (ESI-) ion modes. Samples were mixed in equal amounts to prepare quality control (QC) samples, which were spaced evenly among the injections. All experimental samples were randomly distributed throughout the run in order to monitor the precision and stability of the method during its operation. The raw LC/MS data were converted to mzXML files using Proteo Wizard software. The data were subsequently processed using XCMS for peak detection, alignment, and data filtering [69, 70]. Mass accuracy tolerance within 25 ppm was used as the mass window for the database search and secondary spectral map matching, and the self-built database of the laboratory was retrieved. For the data extracted by XCMS, ion peaks of group sum > 50% were deleted. Pattern recognition was carried out by applying the software SIMCA-P 14.1 (Umetrics, Umea, Sweden).

PLS-DA was performed for the supervised multivariate statistical analysis, and heat maps were generated using a hierarchical clustering algorithm to visualize the metabolite difference within the data set. Single-dimensional statistical analysis includes Student’s *t*-test and multiple of variation analysis. The differential metabolites were submitted to the KEGG website (http://www.genome.jp/kegg/pathway.html) for related pathway analysis.

The correlation matrix between the gut microflora–related metabolites and gut bacterial species was generated using Pearson’s correlation coefficient.

Abbreviations

CITES
Convention on International Trade in Endangered Species of Wild Fauna and Flora; IUCN:International Union for Conservation of Nature; WCM:Wild Chinese monal; CCM:Captive Chinese monal; 16S rRNA:16S ribosomal rRNA; UHPLC:Ultra-high performance liquid chromatograph; OTU:operational taxonomic unit; PLS-DA:Partial least squares discrimination analysis; NCBI:National Center for Biotechnology Information; BLAST:Basic Local Alignment Search Tool; KEGG:Kyoto Encyclopedia of Genes and Genomes; 5-HIAA:5-hydroxyindoleacetic acid.

Declarations

Funding

This work was supported by the Chengdu Giant Panda Breeding Research Foundation (CPF2017-10); and the independent project of Chengdu Research Base of Giant Panda Breeding (2020CPB-C10).

Ethics approval and consent to participate

The experimental protocol was approved by the Chengdu Research Base of Giant Panda

Breeding and in accordance with the current laws on animal welfare and research in China.

Consent for publication

Not applicable.

Availability of data and materials

The datasets used and/or analysed during the current study are available from the corresponding author on reasonable request.

Competing interests

The authors declare that they have no competing interests.

Authors' contributions

HW and RH conceived and designed the study. XH collected samples in the wild. RH and DJ collected samples in the reserve with the help of LC. HW, DJ, XH contributed the measurements and data analysis. DJ wrote the original draft with the help of HW and MV. HW, XH, MV, LC, QX, YY reviewed and edited the manuscript. All authors read and approved the final manuscript.

Acknowledgments

We thank the Shanghai Personal Biotechnology Co., Ltd for the bioinformatics analysis support provided.

Authors' information

Not applicable.

References

1. Wang B, Xu Y, Ran J. Predicting suitable habitat of the Chinese monal (*Lophophorus lhuysii*) using ecological niche modeling in the Qionglai Mountains, China. PeerJ. 2017;5:e3477.
2. Convention on International Trade in Endangered Species of Wild Fauna and Flora. (CITES) Appendices I, II and III. http://www.cites.org. 2016. Accessed 22 March 2022.
3. BirdLife International. *Lophophorus lhuysii. The IUCN Red List of Threatened Species*. 2016: e.T22679192A92806697. https://dx.doi.org/10.2305/IUCN.UK.2016-3.RLTS.T22679192A92806697.en. Accessed 22 March 2022.
4. Zheng G. Pheasants in China: The Chinese monal (*Lophophorus lhuysii*). In: Zheng G, Ding P, Lu X, Zhang Z, Zhang Y, editors.Higher education press, Beijing, China; 2015. p. 338–351.
5. Martin F-PJ, Collino S, Rezzi S, Kochhar S. Metabolomic Applications to Decipher Gut Microbial Metabolic Influence in Health and Disease. Front Physio. 2012;3:113.
6. He F, Zhai J, Zhang L, Liu D, Ma Y, Rong K, et al. Variations in gut microbiota and fecal metabolic phenotype associated with Fenbendazole and Ivermectin Tablets by 16S rRNA gene sequencing and LC/MS-based metabolomics in Amur tiger. Biochem Biophys Res Commun. 2018;499:447–53.
7. Turnbaugh PJ, Ley RE, Mahowald MA, Magrini V, Mardis ER, Gordon JI. An obesity-associated gut microbiome with increased capacity for energy harvest. Nature. 2006;444:1027–31.
8. Wang J, Tang H, Zhang C, Zhao Y, Derrien M, Rocher E, et al. Modulation of gut microbiota during probiotic-mediated attenuation of metabolic syndrome in high fat diet-fed mice. ISME J. 2015;9:1–15.
9. Nelson TM, Rogers TL, Carlini AR, Brown MV. Diet and phylogeny shape the gut microbiota of Antarctic seals: a comparison of wild and captive animals: The gut microbiota of wild and captive Antarctic seals. Environ Microbiol. 2013;15:1132–45.
10. Guan Y, Yang H, Han S, Feng L, Wang T, Ge J. Comparison of the gut microbiota composition between wild and captive sika deer (*Cervus nippon hortulorum*) from feces by high-throughput sequencing. AMB Expr. 2017;7:212.
11. Schmidt E, Mykytczuk N, Schulte-Hostedde AI. Effects of the captive and wild environment on diversity of the gut microbiome of deer mice (Peromyscus maniculatus). ISME J. 2019;13:1293–305.
12. Ushida K, Segawa T, Tsuchida S, Murata K. Cecal bacterial communities in wild Japanese rock ptarmigans and captive Svalbard rock ptarmigans. The Journal of Veterinary Medical Science. 2016;78:251–7.
13. Marcobal A, Kashyap PC, Nelson TA, Aronov PA, Donia MS, Spormann A, et al. A metabolomic view of how the human gut microbiota impacts the host metabolome using humanized and gnotobiotic

mice. ISME J. 2013;7:1933–43.

14. Xie G, Zhang S, Zheng X, Jia W. Metabolomics approaches for characterizing metabolic interactions between host and its commensal microbes: General. ELECTROPHORESIS. 2013;2787–98.
15. Gomez A, Petrzelkova K, Yeoman CJ, Vlckova K, Mrázek J, Koppova I, et al. Gut microbiome composition and metabolomic profiles of wild western lowland gorillas (*Gorilla gorilla gorilla*) reflect host ecology. Mol Ecol. 2015;24:2551–65.
16. Kieffer DA, Piccolo BD, Vaziri ND, Liu S, Lau WL, Khazaeli M, et al. Resistant starch alters gut microbiome and metabolomic profiles concurrent with amelioration of chronic kidney disease in rats. Am J Physiol Renal Physiol. 2016;310:F857–71.
17. Garcia-Mazcorro JF, Pedreschi R, Yuan J, Kawas JR, Chew B, Dowd SE, et al Apple consumption is associated with a distinctive microbiota, proteomics and metabolomics profile in the gut of Dawley Sprague rats fed a high-fat diet. Blachier F, editor. PLoS ONE. 2019;14:e0212586.
18. Scupham AJ, Patton TG, Bent E, Bayles DO. Comparison of the Cecal Microbiota of Domestic and Wild Turkeys. Microb Ecol. 2008;56:322–31.
19. Xenoulis PG, Gray PL, Brightsmith D, Palculict B, Hoppes S, Steiner JM, et al. Molecular characterization of the cloacal microbiota of wild and captive parrots. Vet Microbiol. 2010;146:320–5.
20. Salgado-Flores A, Tveit AT, Wright A-D, Pope PB, Sundset MA. Characterization of the cecum microbiome from wild and captive rock ptarmigans indigenous to Arctic Norway. Chaves AV, editor. PLoS ONE. 2019;14:e0213503.
21. Uenishi G, Fujita S, Ohashi G, Kato A, Yamauchi S, Matsuzawa T, et al. Molecular analyses of the intestinal microbiota of chimpanzees in the wild and in captivity. Am J Primatol. 2007;69:367–76.
22. Gao H, Chi X, Qin W, Wang L, Song P, Cai Z, et al. Comparison of the gut microbiota composition between the wild and captive Tibetan wild ass (*Equus kiang*). J Appl Microbiol. 2019;126:1869–78.
23. Banks JC, Cary SC, Hogg ID. The phylogeography of Adelie penguin faecal flora. Environ Microbiol. 2009;11:577–88.
24. Wilkinson N, Hughes RJ, Aspden WJ, Chapman J, Moore RJ, Stanley D. The gastrointestinal tract microbiota of the Japanese quail, Coturnix japonica. Appl Microbiol Biotechnol. 2016;100:4201–9.
25. Godoy-Vitorino F, Ley RE, Gao Z, Pei Z, Ortiz-Zuazaga H, Pericchi LR, et al. Bacterial Community in the Crop of the Hoatzin, a Neotropical Folivorous Flying Bird. Appl Environ Microbiol. 2008;74:5905–12.
26. Shen J, Zhang X, Wu W, Hu W, Zhang C, Zhu L. The Gut Microbes'Diversity and Function of Phasianidae Provide Insights on the Adaptation to Their Diet. Journal of Nanjing normal university (Natural Science Edition). 2016;39:90–5.
27. Shin N-R, Whon TW, Bae J-W. Proteobacteria: microbial signature of dysbiosis in gut microbiota. Trends Biotechnol. 2015;33:496–503.
28. Koren O, Goodrich JK, Cullender TC, Spor A, Laitinen K, Kling Bäckhed H, et al. Host Remodeling of the Gut Microbiome and Metabolic Changes during Pregnancy. Cell. 2012;150:470–80.

29. Chevalier C, Stojanović O, Colin DJ, Suarez-Zamorano N, Tarallo V, Veyrat-Durebex C, et al. Gut Microbiota Orchestrates Energy Homeostasis during Cold. Cell. 2015;163:1360–74.
30. Sun B, Wang X, Bernstein S, Huffman MA, Xia D-P, Gu Z, et al. Marked variation between winter and spring gut microbiota in free-ranging Tibetan Macaques (Macaca thibetana). Sci Rep. 2016;6:26035.
31. Walker A, Pfitzner B, Neschen S, Kahle M, Harir M, Lucio M, et al. Distinct signatures of host–microbial meta-metabolome and gut microbiome in two C57BL/6 strains under high-fat diet. ISME J. 2014;8:2380–96.
32. Turnbaugh PJ, Hamady M, Yatsunenko T, Cantarel BL, Duncan A, Ley RE, et al. A core gut microbiome in obese and lean twins. Nature. 2009;457:480–4.
33. López-López A, Castellote-Bargalló AI, Campoy-Folgoso C, Rivero-Urgel M, Tormo-Carnicé R, Infante-Pina D, et al. The influence of dietary palmitic acid triacylglyceride position on the fatty acid, calcium and magnesium contents of at term newborn faeces. Early Human Dev. 2001;65:83–94.
34. Certik M, Shimizu S. Biosynthesis and regulation of microbial polyunsaturated fatty acid production. J Biosci Bioeng. 1999;87:1–14.
35. Steen EJ, Kang Y, Bokinsky G, Hu Z, Schirmer A, McClure A, et al. Microbial production of fatty-acid-derived fuels and chemicals from plant biomass. Nature. 2010;463:559–62.
36. Nguyen A, Bouscarel B. Bile acids and signal transduction: Role in glucose homeostasis. Cell Signal. 2008;20:2180–97.
37. Lu K, Abo RP, Schlieper KA, Graffam ME, Levine S, Wishnok JS, et al. Arsenic Exposure Perturbs the Gut Microbiome and Its Metabolic Profile in Mice: An Integrated Metagenomics and Metabolomics Analysis. Environ Health Perspect. 2014;122:284–91.
38. Kim G-B, Lee BH. Biochemical and Molecular Insights into Bile Salt Hydrolase in the Gastrointestinal Microflora - A Review -. Asian Australas J Anim Sci. 2005;18:1505–12.
39. Yeh Y-H, Hwang D-F. High-performance liquid chromatographic determination for bile components in fish, chicken and duck. J Chromatogr B Biomed Sci Appl. 2001;751:1–8.
40. He F, Lu T. Ecology of the Chinese monal in winter. Zoological research. 1985;6:345–52.
41. Long Y, Shao K, Guo G, Cheng C, Zhou X, Hans L, et al. A follow-up study of the ecology of the Chinese monal in winter. Sichuan Journal of Zoology. 1998;17:104–5.
42. Loescher WH, McCamant T, Keller JD. Carbohydrate Reserves, Translocation, and Storage in Woody Plant Roots. HortSci. 1990;25:274–81.
43. Cruz A, Moreno JM. Seasonal Course of Total Non-Structural Carbohydrates in the Lignotuberous Mediterranean-Type Shrub Erica australis. Oecologia. 2001;128:343–50.
44. Knox KJE, Clarke PJ. Nutrient availability induces contrasting allocation and starch formation in resprouting and obligate seeding shrubs. Funct Ecology. 2005;19:690–8.
45. Ridlon JM, Alves JM, Hylemon PB, Bajaj JS. Cirrhosis, bile acids and gut microbiota: Unraveling a complex relationship. Gut Microbes. 2013;4:382–7.

46. Sengupta S, Mukherjee S, Basak P, Majumder AL. Significance of galactinol and raffinose family oligosaccharide synthesis in plants. Front Plant Sci. 2015;6.
47. Iji PA, Saki AA, Tivey DR. Intestinal structure and function of broiler chickens on diets supplemented with a mannan oligosaccharide. J Sci Food Agric. 2001;81:1186–92.
48. Coon CN, Leske KL, Akavanichan O, Cheng TK. Effect of Oligosaccharide-Free Soybean Meal on True Metabolizable Energy and Fiber Digestion in Adult Roosters. Poult Sci. 1990;69:787–93.
49. Martínez del Rio C, Baker HG, Baker I. Ecological and evolutionary implications of digestive processes: Bird preferences and the sugar constituents of floral nectar and fruit pulp. Experientia. 1992;48:544–51.
50. Apanius V. Sucrose Intolerance in Birds: Simple Nonlethal Diagnostic Methods and Consequences for Assimilation of Complex Carbohydrates. Auk. 1994;111:170–7.
51. Lila ZA, Mohammed N, Takahashi T, Tabata M, Yasui T, Kurihara M, et al. Increase of ruminal fiber digestion by cellobiose and a twin strain of Saccharomyces cerevisiae live cells in vitro. Animal Sci J. 2006;77:407–13.
52. Inman DL. Cellulose Digestion in Ruffed Grouse, Chukar Partridge, and Bobwhite Quail. J Wildl Manag. 1973;37:114–21.
53. Wang Y, Yue X, Hu J, Guo Y, Wu X. Morphology of digestive system of *Lophophorus lhuysii*. Journal of China West Normal University (Natural Science). 2007;28:7–10.
54. Lu M, Hashimoto K, Uda Y. Rat intestinal microbiota digest desulfosinigrin to form allyl cyanide and 1-cyano-2,3-epithiopropane. Food Res Int. 2011;44:1023–8.
55. Mokhtari M, Rezaei A, Ghasemi A. Determination of Urinary 5-Hydroxyindoleacetic Acid as a Metabolomics in Gastric Cancer. J Gastrointest Canc. 2015;46:138–42.
56. Degg TJ, Allen KR, Barth JH. Measurement of plasma 5-hydroxyindoleacetic acid in carcinoid disease: an alternative to 24-h urine collections? Ann Clin Biochem. 2000;37:724–6.
57. Sheflin A, Borresen E, Wdowik M, Rao S, Brown R, Heuberger A, et al. Pilot Dietary Intervention with Heat-Stabilized Rice Bran Modulates Stool Microbiota and Metabolites in Healthy Adults. Nutrients. 2015;7:1282–300.
58. Patel D, Patel K, Gadewar M, Tahilyani V. A concise report on pharmacological and bioanalytical aspect of sinigrin. Asian Pacific Journal of Tropical Biomedicine. 2012;2:446–8.
59. Krul C, Humblot C, Philippe C, Vermeulen M, van Nuenen M, Havenaar R, et al. Metabolism of sinigrin (2-propenyl glucosinolate) by the human colonic microflora in a dynamic in vitro large-intestinal model. Carcinogenesis. 2002;23:1009–16.
60. GB/T 6435 – 2014. Determination of moisture in feedstuffs. Beijing: Standards Press of China; 2014.
61. GB/T 6433 – 2006. Determination of crude fat in Feeds. Beijing: Standards Press of China; 2006.
62. GB/T 6432 – 1994. Method for the determination of crude protein in Feedstuffs. Beijing: Standards Press of China; 1994.

63. GB/T 6434 – 2006. Determination of crude fiber in Feeds. Beijing: Standards Press of China; 2006.
64. Magoc T, Salzberg SL. FLASH: fast length adjustment of short reads to improve genome assemblies. Bioinformatics. 2011;27:2957–63.
65. DeSantis TZ, Hugenholtz P, Larsen N, Rojas M, Brodie EL, Keller K, et al. Greengenes, a Chimera-Checked 16S rRNA Gene Database and Workbench Compatible with ARB. AEM. 2006;72:5069–72.
66. Altschul S. Gapped BLAST and PSI-BLAST: a new generation of protein database search programs. Nucleic Acids Res. 1997;25:3389–402.
67. Lozupone C, Knight R. UniFrac: a New Phylogenetic Method for Comparing Microbial Communities. AEM. 2005;71:8228–35.
68. White JR, Nagarajan N, Pop M. Statistical Methods for Detecting Differentially Abundant Features in Clinical Metagenomic Samples. Ouzounis CA, editor. PLoS Comput Biol. 2009;5:e1000352.
69. Ivanisevic J, Epstein AA, Kurczy ME, Benton PH, Uritboonthai W, Fox HS, et al. Brain Region Mapping Using Global Metabolomics Chemistry Biology. 2014;21:1575–84.
70. Benton HP, Ivanisevic J, Mahieu NG, Kurczy ME, Johnson CH, Franco L, et al. Autonomous Metabolomics for Rapid Metabolite Identification in Global Profiling. Anal Chem. 2015;87:884–91.

Figures

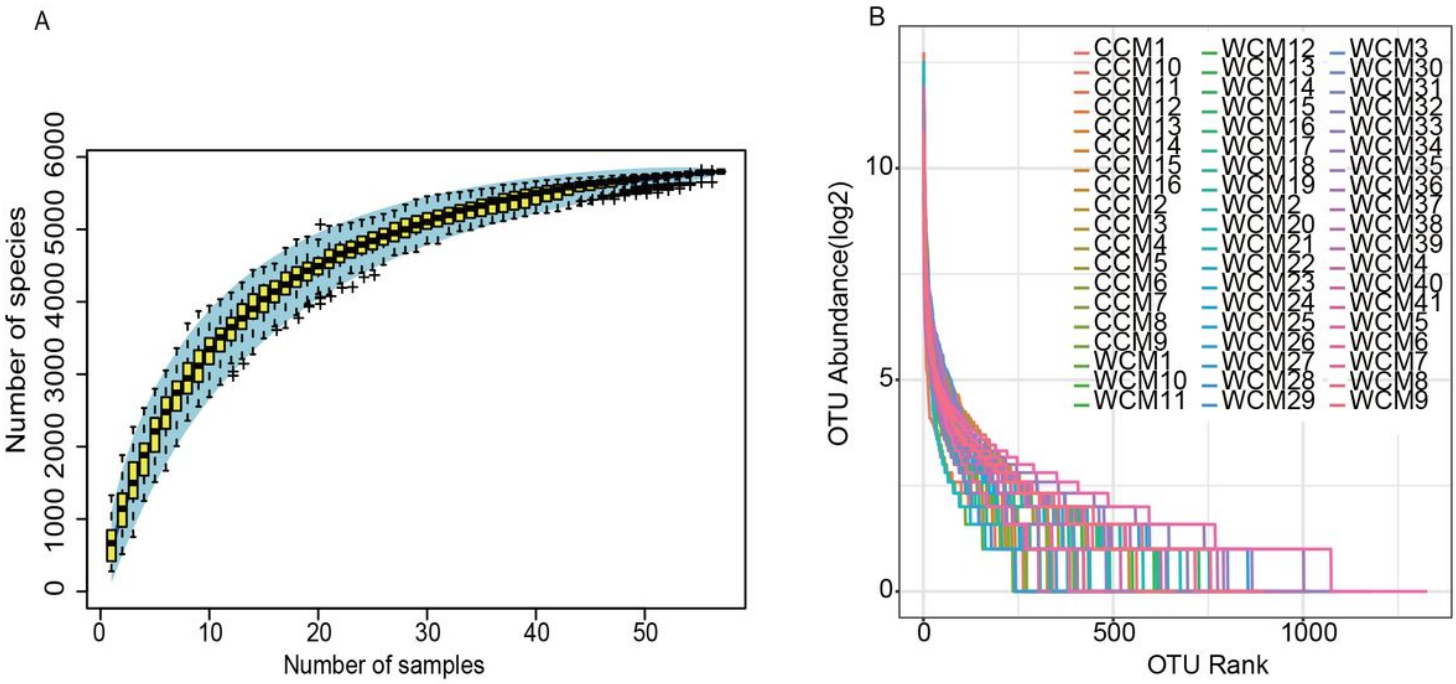

Figure 1

Chinese monal species accumulation curves (A) and rank abundance curve (B).

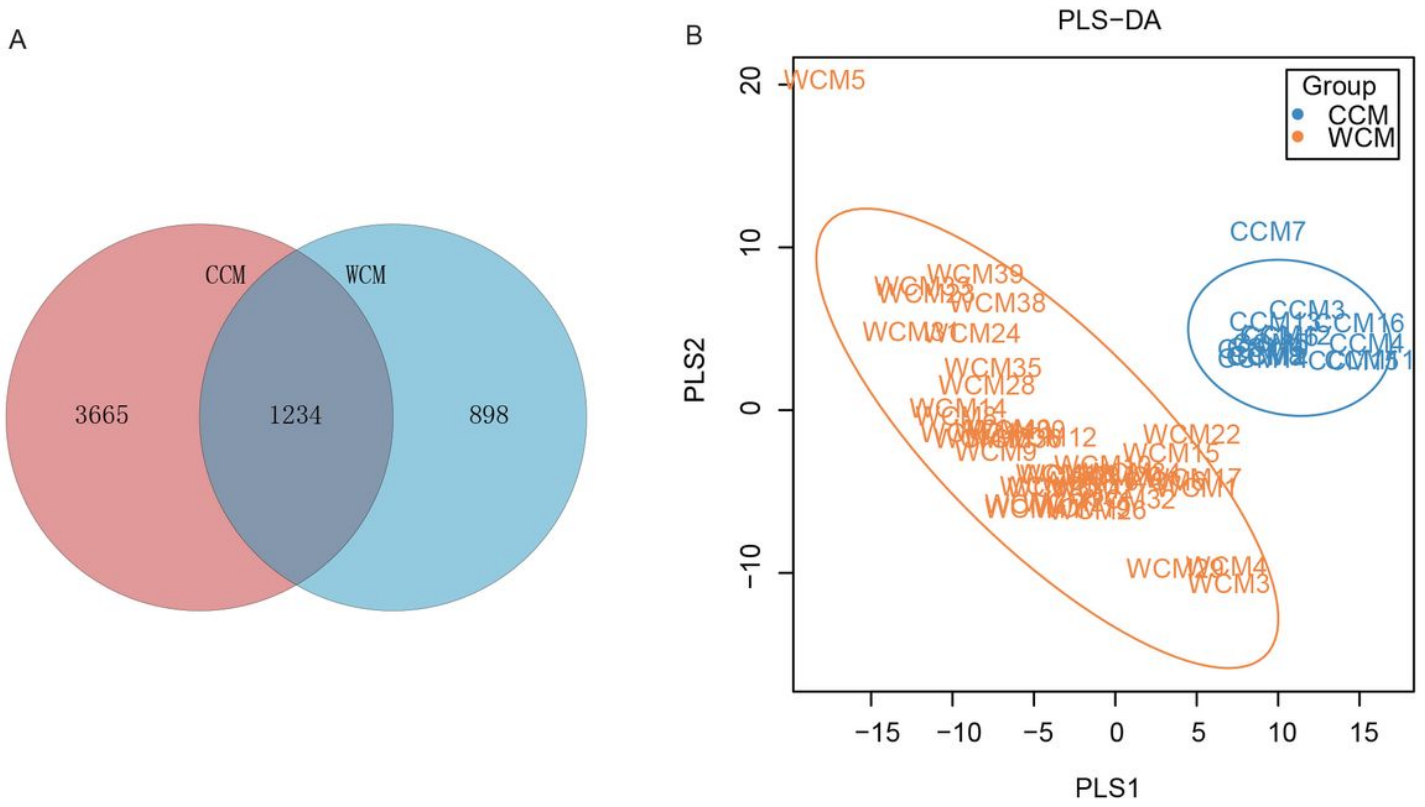

Figure 2

Venn plot (A) and Partial least squares discrimination analysis (PLS-DA) scores scatter plot (B) of fecal microbiome of captive (CCM) and wild Chinese monal (WCM).

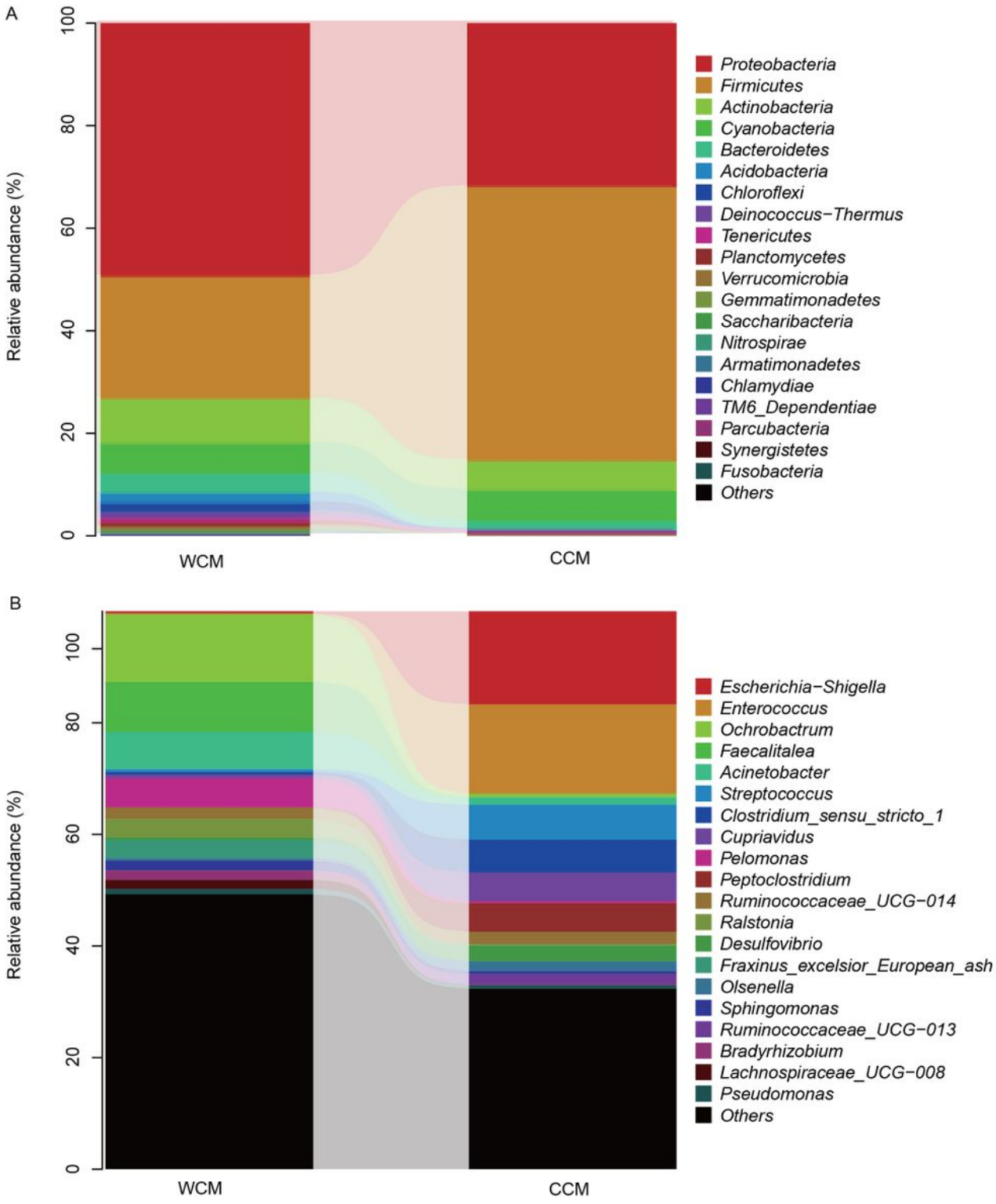

Figure 3

The fecal microbiome composition profiles at the phylum (A) and genus (B) level in the captive (CCM) and wild Chinese monal (WCM).

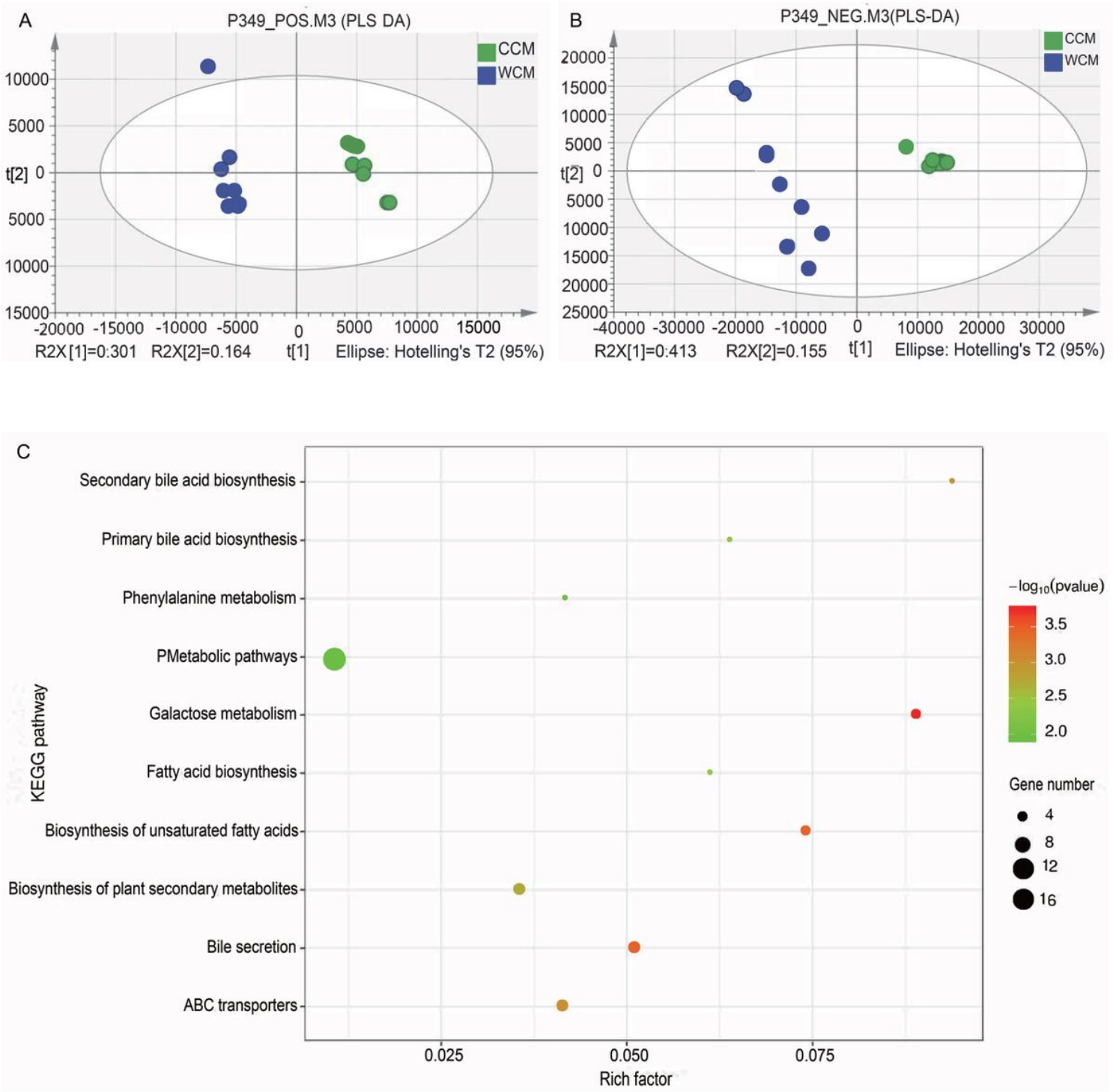

Figure 4

Partial least squares discrimination analysis (PLS-DA) score plots of fecal samples from the captive (CCM) and wild Chinese monal (WCM) group in positive (A) and negative (B) ion modes. KEGG enrichment analysis bubble map display the most significant top 10 enrichment metabolic pathway (C). Rich factor refers to the ratio of the number of significantly different metabolites detected to the number of metabolites annotated in the pathway, and the higher value of rich factor represents greater

enrichment. The size of the point represents the enrichment of significant metabolites in the corresponding metabolic pathway.

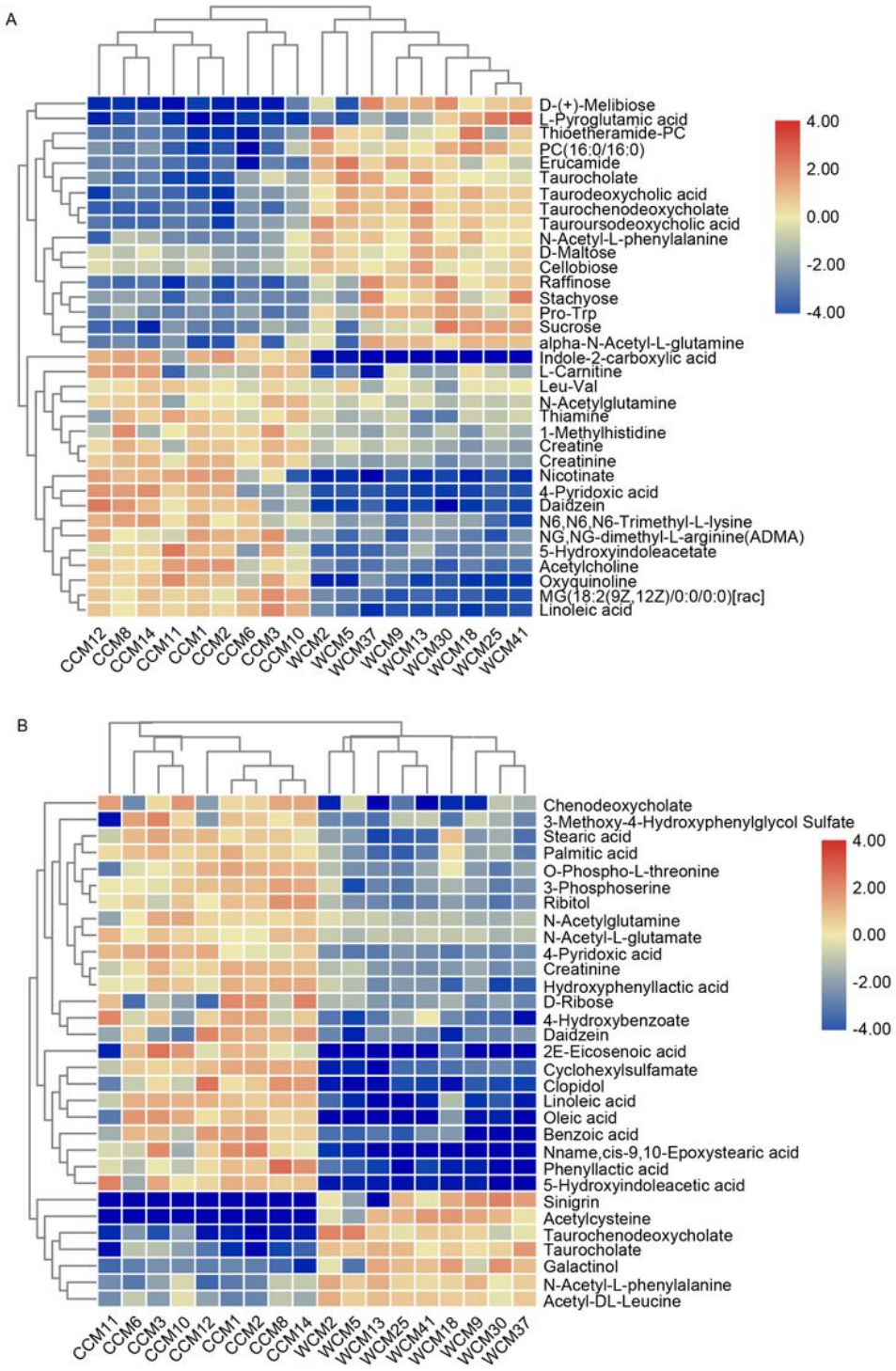

Figure 5

Heat map summarizing fold changes of significantly altered metabolites in the LC/MS data of fecal samples in the positive (A) and negative (B) modes, respectively. Red and blue represent higher and lower concentrations of metabolites in the corresponding abscissa samples, respectively.

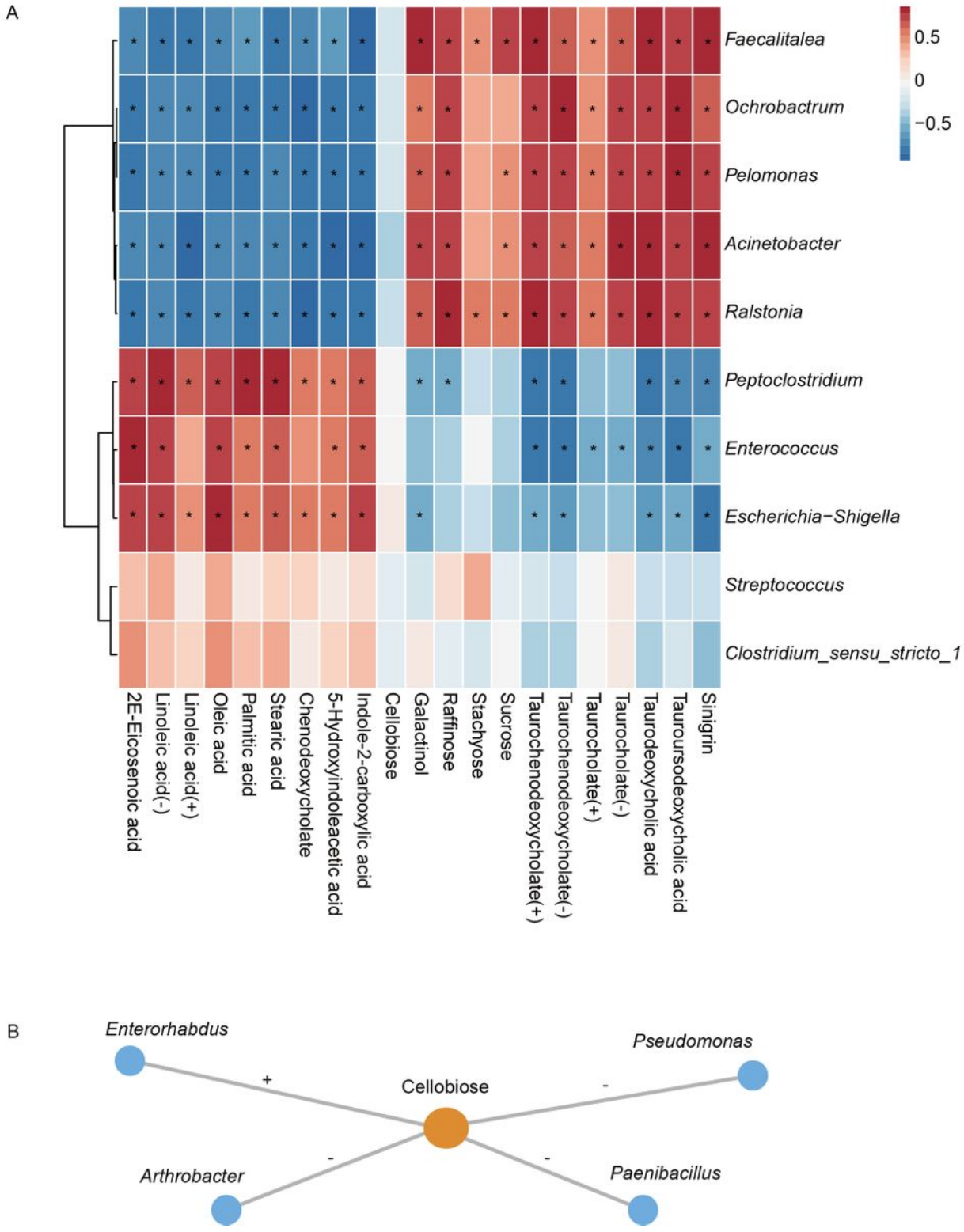

Figure 6

Correlation plot showing the functional correlation between the top 10 most common fecal bacteria genera and specific fecal metabolites(A), and significant correlations between cellobiose and the detected genus(B). Red and blue square represent the positive and negative correlations between metabolites and bacteria, respectively. (+), (-) denote metabolites detected in positive and negative ion modes, respectively.

*, +, - all represent $p < 0.05$, $|r|>0.5$, this means that there are significant correlations between bacteria and metabolites.